eprints@whiterose.ac.uk
https://eprints.whiterose.ac.uk/

Oil-in-Oil Pickering Emulsions Stabilized by Diblock Copolymer Nanoparticles

Matthew J. Rymaruk,[a,]* Victoria J. Cunningham,[b] Steven L. Brown,[b]

Clive N. Williams[b] and Steven P. Armes[a,]*

a. Dainton Building, Department of Chemistry, University of Sheffield, Brook Hill, Sheffield, South Yorkshire, S3 7HF, UK.

b. Scott Bader Company Ltd, Wollaston, Wellingborough, Northamptonshire, NN29 7RL, UK.

Abstract.

Hypothesis. Diblock copolymer nanoparticles have been shown to be Pickering emulsifiers for both oil-in-water and water-in-oil emulsions. Recently, we reported the preparation of sterically-stabilized diblock copolymer spheres in a low-viscosity silicone oil (Macromolecules 53 (2020) 1785-1794). We hypothesized that such spheres could be used as a Pickering emulsifier for a range of oil-in-oil emulsions comprising droplets of a bio-sourced oil dispersed in silicone oil.

Experiments. Diblock copolymer spheres were prepared via reversible addition-fragmentation chain transfer (RAFT) dispersion polymerization of benzyl methacrylate in silicone oil and characterized by dynamic light scattering and transmission electron microscopy. These spheres were evaluated as Pickering emulsifiers for a series of oil-in-oil Pickering emulsions. The influence of both sphere size and core-forming block composition was investigated.

Findings. Optimization of the nanoparticle size and core-forming block composition enabled stable bio-sourced oil-in-silicone emulsions to be obtained for nine out of the ten bio-sourced oils investigated. These emulsions were characterized in terms of their mean droplet size by optical microscopy.

Key Words: Pickering emulsions, Nanoparticles, Block copolymers, Self-assembly,

* Authors to whom correspondence should be addressed (m.rymaruk@shef.ac.uk or

s.p.armes@shef.ac.uk)

Introduction. It is well known that generation of an interface between two immiscible fluids is energetically unfavorable.[1] Thus, the total surface free energy can be minimized by reducing the interfacial area for each fluid, which leads to the phenomenon of interfacial tension.[2] This means that emulsification, which produces droplets of one liquid dispersed in a second immiscible liquid, produces an inherently unstable system. Hence a suitable stabilizer, typically a surfactant, is required to produce emulsions that exhibit long-term stability.[2–8] Surfactants stabilize fluid interfaces via adsorption, which reduces the interfacial energy.[9,10] Such amphiphiles enable the formation of long-lived oil-in-water emulsions,[11] water-in-oil emulsions,[12] non-aqueous emulsions[13] and aqueous foams.[14,15]

In the early 1900s Ramsden and Pickering independently reported that various types of colloidal particles can also stabilize fluid interfaces.[16,17] For particles, adsorption reduces the interfacial area and hence lowers the free energy of the system.[5] Furthermore, unlike surfactants, such particles need not be amphiphilic – the only requirement is that they should be partially wetted by both fluids.[5,18,19] This criterion is fulfilled by many types of inorganic and organic particles, such as silica,[20–22] titania,[23] calcium carbonate,[24] clays,[25,26] barium sulfate,[27] iron oxide,[28] graphene oxide,[29] carbon black,[30] cellulose nanocrystals,[31–33] latexes,[34,35] microgels,[36,37] etc. After many decades of relative inactivity, there has been a resurgence of interest in Pickering emulsions over the past twenty years or so.[19] Consequently, there are now many literature examples of oil-in-water Pickering emulsions.[38–41] These have been prepared using a wide range of particles[27,33,36,39,42–47] of varying size[34,46,48] and morphology.[31,33,49,50] Similarly, water-in-oil Pickering emulsions have also been explored by various research groups.[32,51–54] However, there are far fewer reports of oil-in-oil emulsions stabilized by nanoparticles.[55–59] In some of these examples, one of the 'oils' is relatively polar, e.g. DMF,[58] alcohol,[60,61] or glycerol, which no doubt promotes immiscibility.[62,63] However, various research groups have reported that both oils can be liquids with low relative permittivities ($\varepsilon_r < 5.0$).[55–57,64–67]

Oil-in-oil Pickering emulsions have been evaluated for lubricant and cosmetics applications.[55]

Indeed, most reports of oil-in-oil Pickering emulsions appear in the patent literature, dating back as

far as the 1960s.[55] Generally, such examples comprise a silicone oil and either a mineral oil or a

bio-sourced oil. There are also a few reports of oil-in-oil Pickering emulsions in the academic

literature. For example, Binks and co-workers demonstrated that emulsions comprising

polydimethylsiloxane (PDMS, viscosity = 20-100 cSt) combined in turn with olive oil, sunflower oil or

rapeseed oil can be prepared using surface-modified fumed silica particles.[55] Furthermore, such

silica particles also enabled the production of oil-in-oil-in-oil double emulsions.[56] More recently,

Rozynek and co-workers reported that silicone oil droplets can be stabilized within castor oil using

various Pickering emulsifiers, including dyed polyethylene, polystyrene or silica particles.[57,64,65]

Moreover, applying an electric field to such emulsions enabled their coalescence behavior to be

controlled, thus producing a relatively narrow droplet size distribution compared to emulsions

prepared using conventional techniques.[57,68]

Recently, we reported the preparation of a range of poly(3-[tris(trimethylsiloxy)silyl]propyl

methacrylate)-poly(benzyl methacrylate) (PSiMA-PBzMA) nanoparticles in a low-viscosity, *cyclic*

silicone oil (decamethylcyclopentasiloxane or D5).[69] This was achieved by reversible addition-

fragmentation chain transfer (RAFT) dispersion polymerization, which is an example of

polymerization-induced self-assembly (PISA). In the current study, we prepare similar PSiMA-PBzMA

spheres directly in a low-viscosity *linear* silicone oil (dimethicone 5 or DM5, which has a solution

viscosity of 5 cSt), see **Scheme 1**. Importantly, DM5 is immiscible with many common bio-sourced

oils such as sunflower oil, whereas D5 is miscible with such oils. Thus we hypothesized that these

sterically-stabilized nanoparticles might serve as putative Pickering emulsifiers for the stabilization of

bio-sourced oil droplets within a continuous phase comprising DM5. This concept is explored herein

for ten bio-sourced oils. Importantly, it is shown that statistical copolymerization of lauryl

methacrylate (LMA) with benzyl methacrylate (BzMA) within the nanoparticle cores significantly

enhances Pickering emulsifier performance, enabling stabilization of a much wide range of bio-sourced oil-in-DM5 emulsions.
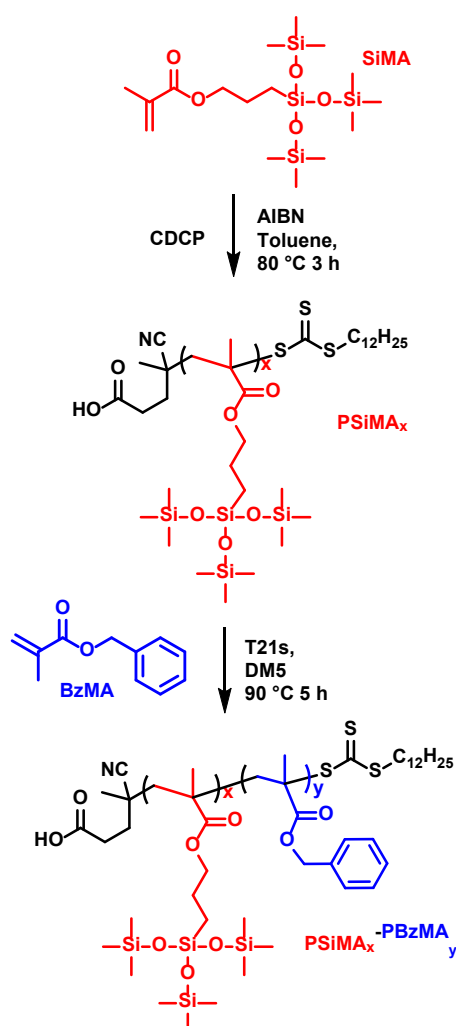
Scheme 1. Reaction scheme for the RAFT solution polymerization of SiMA in toluene at 80 °C using a CDCP RAFT agent followed by the RAFT dispersion polymerization of BzMA at 90 °C in silicone oil (DM5).

Experimental section

Materials. 4-Cyano-4-(((dodecylthio)carbonothioyl)thio)pentanoic acid (CDCP) was purchased from Boron Molecular (Australia). SiMA monomer was obtained from TER (Cambridge, UK). Lauryl methacrylate (LMA), benzyl methacrylate (BzMA), 1-pyrenemethanol, 4-dimethylaminopyridine (DMAP), N,N'-dicyclohexylcarbodiimide (DCC), dichloromethane, CDCl$_3$, CD$_2$Cl$_2$, castor oil and linseed

oil were obtained from Sigma Aldrich (UK). Tall oil fatty acid (TOFA 2%), tall oil fatty acid (TOFA 26%), argan oil, pumpkin seed oil, jojoba oil, macadamia oil, 2,2'-azobisisobutyronitrile (AIBN) and Trigonox 21s (T21s) initiator were provided by Scott Bader Ltd. (Wollaston, UK). Olive oil and sunflower oil were purchased from Co-Op Food Ltd. (UK). DM5 (5 cSt) was obtained from Bluestar Silicones (USA). Anhydrous dichloromethane was obtained from an in-house Grubbs dry solvent system. LMA was passed through basic alumina prior to use, while all other reagents were used as received.

Methods

Synthesis of the PSiMA hompolymer precursor. A typical synthesis was conducted as follows: SiMA monomer (20.95 g, 49.55 mmol) and toluene (32.70 g) were weighed into a round-bottomed flask. CDCP RAFT agent (0.80 g, 1.98 mmol) and AIBN initiator (0.10 g, 0.66 mmol) were added in order to target a PSiMA DP of 25 using a CDCP/AIBN molar ratio of 3.0. The flask was then sealed, cooled (using an ice bath) and the reaction solution was purged with nitrogen for 30 min. The flask was then placed in a pre-heated oil bath at 80 °C for 3 h, after which the polymerization was quenched by cooling the flask to 0 °C and exposing its contents to air. ^{1}H NMR spectroscopy studies conducted in CDCl$_3$ indicated a SiMA conversion of 80%. The resulting mixture was purified by precipitation into a ten-fold excess of methanol (three times) and then dried under high vacuum. End-group analysis via UV spectroscopy in chloroform indicated a mean PSiMA DP of 19.

Synthesis of PSiMA$_{19}$-PBzMA$_x$ nanoparticles via RAFT dispersion polymerization of BzMA in DM5

A typical synthesis of PSiMA$_{19}$-PBzMA$_x$ nanoparticles in DM5 was conducted as follows. The PSiMA$_{19}$ precursor (0.38 g, 45.3 µmol), BzMA (1.60 g, 9.0 mmol; target DP = 200) and DM5 (7.92 g) were added to a round-bottomed flask equipped with a magnetic flea. The reaction solution was stirred for 1 h at 20 °C, or until all of the PSiMA$_{19}$ precursor had dissolved. T21s initiator was then added (9.0 µmol, added as a 10% v/v solution in DM5) and the flask was sealed, before degassing the reaction solution with nitrogen for 30 min. The flask was then immersed in a pre-heated oil bath at 90 °C for 5 h. The resulting dispersions were obtained as free-flowing fluids, which were either turbid or

transparent depending on the target DP for the PBzMA block. ^{1}H NMR spectroscopy studies conducted in CDCl$_3$ confirmed that more than 99% BzMA conversion was achieved in each case.

Synthesis of PSiMA$_{19}$-P(BzMA$_x$-*stat*-LMA$_y$) nanoparticles via RAFT dispersion copolymerization of BzMA and LMA in DM5

A typical synthesis of PSiMA$_{19}$-P(BzMA$_{175}$-*stat*-LMA$_{25}$) nanoparticles in DM5 was conducted as follows. BzMA (0.88 g, 4.98 mmol), LMA (0.18 g, 0.71 mmol) DM5 (5.19 g) and PSiMA precursor (0.24 g, 28.45 µmol; target core-forming block DP = 200), were added to a round-bottomed flask equipped with a magnetic flea. This solution was stirred for 1 h, or until all of the PSiMA precursor had dissolved. T21s initiator was then added (5.6 µmol, added as a 10% v/v solution in DM5) to the reaction mixture and the flask was sealed, purged with nitrogen for 30 min, and finally immersed in a pre-heated oil bath at 90 °C for 5 h. The resulting dispersions were obtained as a turbid free-flowing fluid. ^{1}H NMR spectroscopy confirmed that more than 99% monomer conversion was achieved in each case. In order to vary the LMA content, the same overall target DP of 200 was targeted at a fixed copolymer concentration of 20% w/w solids and the relative proportions of the LMA and BzMA comonomers were varied with all other parameters being held constant.

Synthesis of a pyrene-labeled PSiMA$_{19}$ precursor

PSiMA$_{19}$ precursor (1.00 g, 118 µmol) was weighed into a flame-dried round-bottomed flask and placed under an inert nitrogen atmosphere. 1-Hydroxymethylpyrene (55.0 mg, 237 µmol) and DMAP (2.10 mg, 17.78 µmol) were then co-dissolved in anhydrous CH$_2$Cl$_2$ (10 ml) and this solution was added *via* syringe. The resulting reaction mixture was cooled to 0 °C for 30 min and a solution of DCC (73.25 mg, 355 µmol, dissolved in 5 ml CH$_2$Cl$_2$ prior to addition) was added dropwise over 30 min. The resulting mixture was allowed to warm up to ambient temperature, before being heated at 30 °C. for 18 h. The reaction solution was then exposed to air and cooled in a freezer set at −17 °C overnight. A white precipitate gradually formed, which was removed *via* filtration. The product was then purified by precipitation into excess methanol (five times). ^{1}H NMR spectroscopy studies

indicated a degree of esterification of approximately 30 % by comparing the integrated pyrene signals at around 8 ppm to that of the oxymethylene protons of the SiMA repeat units at 4.5 ppm.

Synthesis of pyrene-labeled PSiMA$_{19}$-PBzMA$_{200}$ nanoparticles

The preparation of pyrene-labeled PSiMA$_{19}$-PBzMA$_{200}$ nanoparticles in DM5 was conducted as follows. The pyrene-labeled PSiMA precursor (0.30 g, 34.6 μmol; mean degree of esterification = 30%) was added to a round-bottomed flask equipped with a magnetic flea. DM5 (6.08 g) and BzMA (1.22 g, 6.92 mmol) were then added to target a PBzMA core-forming DP of 200. The reaction solution was stirred for 1 h, or until all of the precursor had dissolved. T21s initiator (1.5 mg, 7.0 μmol) was then added as a 10% v/v solution in DM5 and the reaction mixture was sealed, purged with nitrogen for 30 min and immersed in a pre-heated oil bath at 90 °C for 5 h. The resulting copolymer dispersion was obtained as a free-flowing fluid. ^{1}H NMR spectroscopy studies confirmed that more than 99% BzMA conversion was achieved and DLS studies (see below) indicated a z-average diameter of 95 nm.

Preparation of Pickering emulsions

Pickering emulsions were prepared via high-shear homogenization using a Silverson L4RT high-shear mixer at 7 500 rpm for 2 min at 20 °C. Unless otherwise stated, the oil volume fraction was 0.50 in each case.

Preparation of fluorescent Pickering emulsions

A typical preparation of a fluorescent Pickering emulsion was conducted as follows. DM5 (4.0 ml) containing 0.75% w/w PSiMA$_{19}$-PBzMA$_{200}$ nanoparticles was added to castor oil (4.0 ml). The resulting mixture was then homogenized for 2 min at 7 500 rpm using a Silverson L4RT high-shear mixer. Over the course of 1 h, droplet sedimentation occurred owing to the density difference between the castor oil (droplet phase) and the DM5 (continuous phase). The DM5 layer containing excess non-adsorbed fluorescent nanoparticles was removed *via* pipet and replaced with fresh DM5.

The emulsion was then gently hand-shaken to redisperse the droplets and this protocol was repeated four more times to ensure complete removal of the non-adsorbed fluorescent nanoparticles from the continuous phase prior to fluorescence microscopy studies.

Characterization

^{1}H NMR spectroscopy

^{1}H NMR spectra were recorded at 25 °C using a Magnitrek Spinsolve bench-top instrument operating at 60 MHz. For characterization of the pyrene-labeled PSiMA$_{19}$ precursor, a Bruker AV1-400 MHz spectrometer was used. Typically, 64 scans were averaged per spectrum.

Gel permeation chromatography

Molecular weight distributions were determined at 30 °C using a GPC set-up comprising two Polymer Laboratories PL gel 5 μm Mixed C columns, a LC20AD ramped isocratic pump, THF eluent and a WellChrom K-2301 refractive index detector operating at 950 ± 30 nm. The mobile phase contained 2.0% v/v triethylamine and 0.05% w/v 3,5-di-tert-4-butylhydroxytoluene (BHT); the flow rate was 1.0 ml min^{-1} and toluene was used as a flow rate marker. A series of ten near-monodisperse poly(methyl methacrylate) standards (M$_p$ = 1 280 to 330 000 g mol^{-1}) were used for calibration. Chromatograms were analyzed using Varian Cirrus GPC software.

Dynamic light scattering

DLS studies of the diblock copolymer nanoparticles were performed using a Zetasizer Nano-ZS instrument (Malvern Instruments, UK) at 25 °C at a scattering angle of 173° and a copolymer concentration of ~ 0.2% w/w. The z-average diameter (which is an intensity-weighted mean diameter reported by DLS) and polydispersity (PDI) were calculated by cumulants analysis of the experimental correlation function using Dispersion Technology Software version 6.20. Data were averaged over ten runs each of thirty seconds duration.

UV spectroscopy

UV spectra were recorded at 25 °C using a PC-controlled UV-1800 spectrophotometer equipped with a 1.0 cm quartz cell. A Beer–Lambert calibration curve was constructed using a series of twelve CDCP stock solutions of known concentration in chloroform. The absorption maximum at 312 nm assigned to the trithiocarbonate end-group was used for this calibration plot, with CDCP concentrations ranging from 10 μmol dm^{-3} to 80 μmol dm^{-3}. The mean DP for each PSiMA$_{19}$ macro-CTA was calculated using a molar extinction coefficient of 11 460 ± 229 mol^{-1} dm^3 cm^{-1} determined for CDCP.

Density measurements

Oil densities were determined using an Anton Paar DMA 4100 M density meter operating at 25 °C.

Transmission electron microscopy

Transmission electron microscopy (TEM) studies were conducted using a FEI Tecnai G2 spirit instrument operating at 80 kV and equipped with a Gatan 1k CCD camera. Copper TEM grids were surface-coated in-house to yield a thin film of amorphous carbon. The grids were then loaded with one droplet of a 0.20% w/w copolymer dispersion using a micropipet. Prior to imaging, each grid was exposed to ruthenium(IV) vapor for 7 min at 20 °C in order to improve contrast. The ruthenium(IV) oxide stain was prepared by adding ruthenium(II) oxide (0.30 g) to water (50 g) in order to form a slurry. Then, sodium periodate (2.0 g) was added with vigorous stirring to form a yellow solution of ruthenium(IV) oxide within 1 min.[70]

Optical microscopy

Optical microscopy images were recorded using a Zeiss Axio Scope A1 microscope and analyzed using ArcSoft ShowBiz software - version 3.5.15.67. Mean droplet diameters were determined *via* image analysis using ImageJ software. At least 100 droplets were imaged in each case.

Fluorescence microscopy

Fluorescence microscopy images were recorded using a Zeiss Axio Scope A1 microscope equipped with an AxioCam 1Cm1 monochrome camera fitted with Zeiss filter set 43 HE (excitation 550/25 nm and emission 605/70 nm). Images were captured and processed using ZEN lite 2012 software.

Surface tensiometry.

Interfacial tension was measured at 20 °C using a Kruss K10 instrument equipped with a Du Noüy ring.

Results and discussion

A PSiMA precursor with a mean DP of 19 was prepared *via* RAFT solution polymerization of SiMA in toluene using a commercially available RAFT agent CDCP, according to **Scheme 1**. The polymerization was quenched at around 80% SiMA conversion (as indicated by ^{1}H NMR studies) to preserve the RAFT chain-ends. The mean DP for the purified precursor was determined to be 19 by UV spectroscopy by constructing a linear Beer-Lambert calibration curve for the strong $\pi - \pi^*$ absorption band at λ = 312 nm (see **Figure S1**). Furthermore, THF GPC analysis (refractive index detector, poly(methyl methacrylate) calibration standards) indicated an M_n of 6 200 g mol^{-1} and an M_w/M_n of 1.16, indicating good RAFT control.

In order to prepare well-defined diblock copolymer nanoparticles, the PSiMA precursor block was then chain-extended via RAFT dispersion polymerization of BzMA at 90 °C targeting 20% w/w solids in DM5 (see **Scheme 1**). In each case, the PBzMA target DP was either 50 or 200. Thus, two examples of PSiMA$_{19}$-PBzMA$_x$ nanoparticles were prepared, as summarized in **Table 1**.

Table 1. Summary of characterization data obtained for the two types of PSiMA$_{19}$-PBzMA$_y$ diblock copolymer nanoparticles used in this study, including BzMA conversion, number-average molecular weight (M_n), dispersity (M_w/M_n), and the z-average diameter (d_z) and corresponding polydispersity index (PDI) obtained from DLS studies.

PSiMA DP	Target PBzMA DP	Conversion[a] / %	Diblock Copolymer Composition	THF GPC		DLS	
				M_n / g mol^{-1}	M_w/M_n	d_z / nm	PDI
19	50	> 99	PSiMA$_{19}$-PBzMA$_{50}$	11,200	1.29	30	0.04
19	200	> 99	PSiMA$_{19}$-PBzMA$_{200}$	40,500	3.30	123	0.08

a. Determined by ^{1}H NMR spectroscopy studies.

^{1}H NMR spectroscopy studies indicated that more than 99 % BzMA conversion was achieved within 2 h for both PISA syntheses. TEM images confirmed that a spherical morphology was obtained in each case (see **Figure 1**), while DLS studies indicated relatively narrow size distributions (PDI < 0.10). It is perhaps noteworthy that the apparent nanoparticle aggregation indicated by TEM is most likely a drying artefact because DLS studies do not indicate any flocculation for the diluted dispersions.
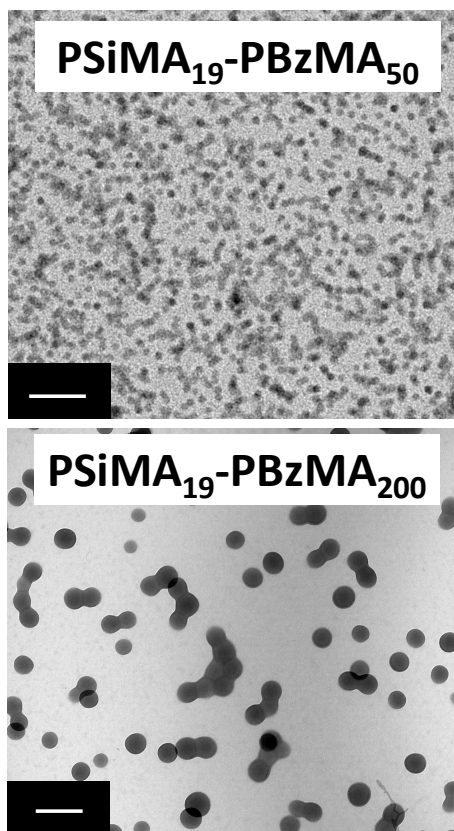

Figure 1. TEM images recorded for $PSiMA_{19}$-$PBzMA_x$ spherical nanoparticles (where x = 50 or 200). In each case the scale bar corresponds to 200 nm.

To produce oil-in-oil Pickering emulsions, a second oil that is immiscible with DM5 is required. To identify suitable oils, a range of bio-sourced oils were examined. In each case, 4.0 ml DM5 and 4.0 ml of the bio-sourced oil were homogenized under high shear at 7 500 rpm for 2 min at 20 °C. The resulting emulsions were then allowed to stand for 24 h prior to visual inspection. The digital photograph in **Figure 2** indicates the ten oils that proved to be sufficiently immiscible with DM5.
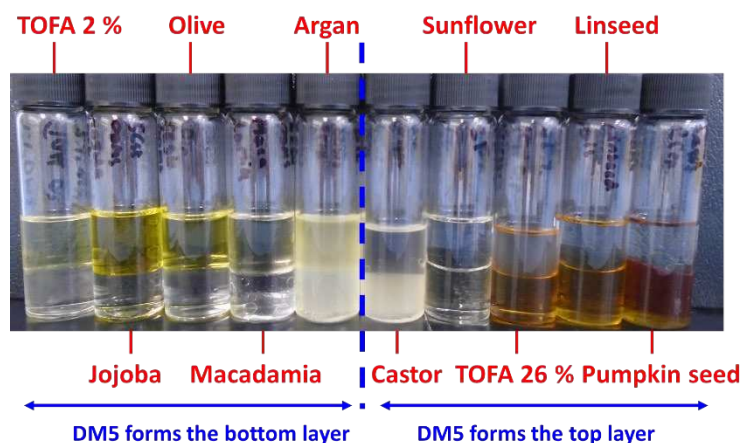
Figure 2. Digital photograph recorded 24 h after high shear homogenization of equal volumes of DM5 with a range of bio-sourced oils (see labels; 'TOFA' denotes tall oil fatty acid and the % value indicates its rosin acid content). For the five vials shown on the left-hand side, DM5 is the denser phase and hence forms the lower layer. For the five vials shown on the right-hand side, DM5 is the less dense phase and hence forms the upper layer.

For each oil/DM5 pair, the interfacial tension was then measured using the Du Noüy ring method (see **Table S1**). In all cases, the measured interfacial tension was below 4.4 mN m^{-1}. In preliminary experiments to determine which of the two types of PSiMA$_{19}$-PBzMA$_x$ spherical nanoparticles was the most effective Pickering emulsifier, each copolymer dispersion was evaluated using only three of the ten oils shown in **Figure 2**, specifically argan, sunflower and castor oil. In these preliminary scoping experiments, 4.0 ml of the desired 2% w/w copolymer dispersion in DM5 was added to 4.0 ml of each bio-sourced oil prior to high shear homogenization of this binary oil mixture at 7 500 rpm for 2 min. The initial emulsions were then allowed to stand for two weeks at 20 °C before visual inspection and optical microscopy analysis. The PSiMA$_{19}$-PBzMA$_{50}$ spheres formed stable emulsions with castor oil, whereas the initial emulsions prepared using sunflower or argan oil underwent complete phase separation over the course of two weeks, see **Figure 3**. However, the larger PSiMA$_{19}$-PBzMA$_{200}$ spheres produced Pickering emulsions that remained stable for at least two weeks when using either sunflower, argan or castor oil. Optical microscopy studies revealed the presence of well-defined spherical droplets in each case. Furthermore, each emulsion was readily dispersible in DM5, indicating that this oil formed the continuous phase. It is perhaps noteworthy

that castor oil has a significantly greater density (ρ = 0.96 g cm^{-3}) than DM5 (ρ = 0.92 g cm^{-3}), see

Table S2. Hence castor oil droplets in DM5 undergo sedimentation on standing. However, these

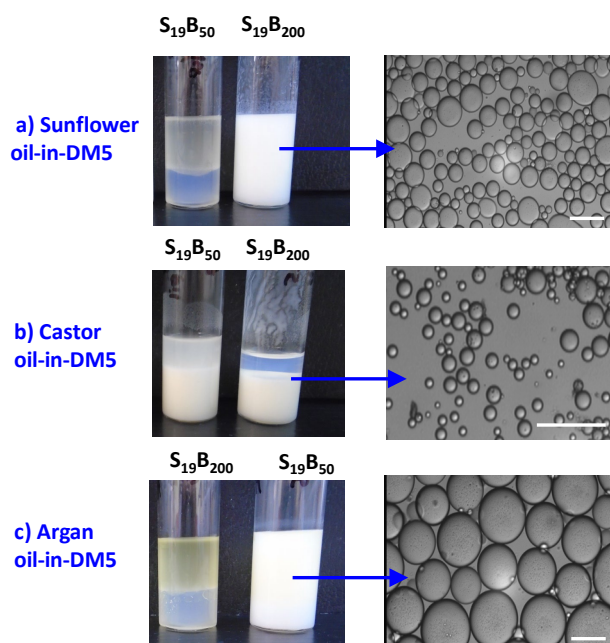droplets remain stable towards coalescence and can be readily redispersed by gentle hand-shaking.

Figure 3. Digital photographs recorded after storage for two weeks at 20 °C for a series of Pickering emulsions prepared using PSiMA$_{19}$-PBzMA$_x$ nanoparticles (where x = 50 or 200), (a) sunflower oil-in-DM5, (b) castor oil-in-DM5 and (c) argan oil-in-DM5. For each emulsion, a 2.0% w/w nanoparticle dispersion in DM5 was utilized, and the DM5 volume fraction was fixed at 0.50. Optical micrographs are also shown for the three PSiMA$_{19}$-PBzMA$_{200}$ stabilized emulsions. The scale bar corresponds to 100 µm in each case. For brevity, S denotes PSiMA and B denotes PBzMA when referring to each diblock composition.

Conversely, argan oil (ρ = 0.91 g cm^{-3}) and sunflower oil (ρ = 0.92 g cm^{-3}) have approximately the

same density as DM5. Thus these droplets underwent minimal sedimentation or creaming on

standing for two weeks at 20 °C Presumably, the superior Pickering emulsifier performance exhibited

by the PSiMA$_{19}$-PBzMA$_{200}$ spheres is related to their size – such nanoparticles are significantly larger

than the PSiMA$_{19}$-PBzMA$_{50}$ spheres (123 nm vs. 30 nm diameter, see **Table 2**). It is well-known that

the energy of detachment of a spherical nanoparticle located at a fluid interface is proportional to

the square of its radius, with larger nanoparticles being adsorbed much more strongly than smaller

ones.[5] In view of these initial experiments, only PSiMA$_{19}$-PBzMA$_{200}$ nanoparticles were used for

further studies. Next, a series of Pickering emulsions were prepared using each of the ten oils shown in **Figure 2** in turn. PSiMA$_{19}$-PBzMA$_{200}$ spheres were used as a Pickering emulsifier at 2.0% w/w copolymer concentration. The DM5 volume fraction was fixed at 0.50 in each case and each emulsion was homogenized at 7 500 rpm for 2 min. After two months standing at 20 °C, sunflower oil-in-DM5, castor oil-in-DM5 and TOFA 26 % oil-in-DM5 Pickering emulsions remained stable towards coalescence, as indicated by optical microscopy (**Figure 4**). Sedimentation was observed for the latter two emulsions because each bio-sourced oil is denser than DM5, but in both cases redispersion was readily achieved by gentle hand-shaking. Conversely, no significant creaming or sedimentation was observed when using sunflower oil as the dispersed phase because it has approximately the same density as DM5. Emulsions prepared with TOFA 2%, argan, macadamia, olive and linseed oil exhibited initial stability, but phase separation occurred within 2-3 weeks of standing at 20 °C. On the other hand, emulsions prepared with jojoba or pumpkin seed oil proved to be unstable, with macroscopic phase separation occurring almost immediately.
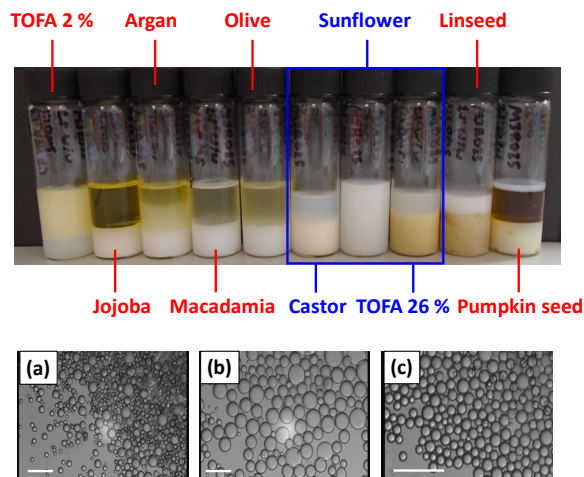

Figure 4. Digital photograph recorded after standing for two months at 20 °C showing various bio-sourced oil-in-DM5 Pickering emulsions prepared using a 2.0% w/w dispersion of PSiMA$_{19}$-PBzMA$_{200}$ spheres in DM5. Each specific oil is indicated above or below the relevant vial: emulsions that remained stable after two months are denoted in blue, whereas those that undergo (partial) phase separation are shown in red. Corresponding optical micrographs are also shown for (a) castor oil-in-DM5, (b) sunflower oil-in-DM5 and (c) TOFA 26% oil-in-DM5 Pickering emulsions prepared using this protocol. In each case the scale bar corresponds to 100 μm

One concern when preparing such Pickering emulsions is that nanoparticle dissociation might occur under high shear, resulting in the adsorption of individual diblock copolymer chains at the oil-oil interface. For example, such *in situ* dissociation has been observed by Thompson and co-workers when attempting to prepare *n*-dodecane-in-water emulsions using linear PGMA-PHPMA spheres.[49] However, dissociation was not observed in this prior study if the weakly hydrophobic core-forming PHPMA block was replaced with a much more hydrophobic block such as PBzMA. Nevertheless, given the possibility of nanoparticle dissociation occurring under shear, the three stable oil-in-oil emulsions prepared using castor oil, sunflower oil or TOFA 26% were further evaluated to examine whether they were genuine Pickering emulsions or not. Thus the PSiMA$_{19}$-PBzMA$_{200}$ concentration used to prepare these emulsions was systematically varied to investigate how this parameter affected the mean droplet diameter. The diameter of the freshly-prepared emulsions were then determined via optical microscopy (see **Figure 5**).
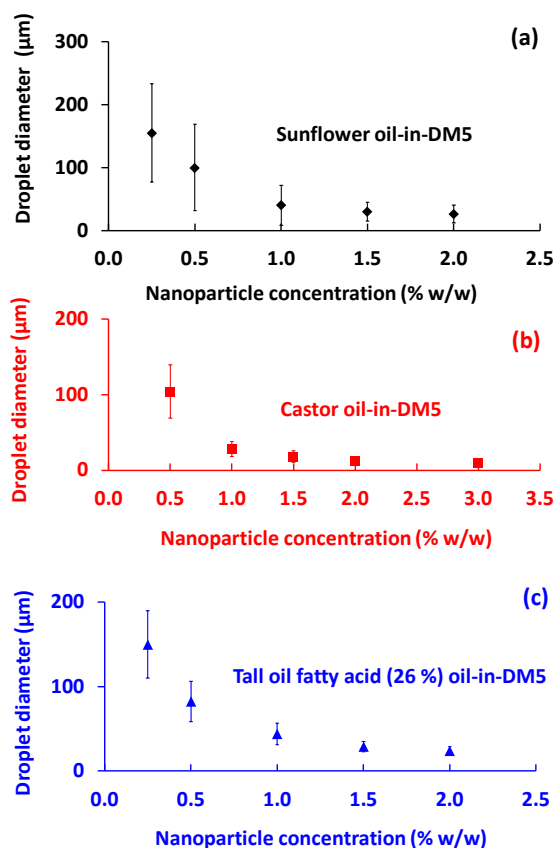
Figure 5. Variation in the mean droplet diameter with nanoparticle concentration for (a) sunflower oil-in-DM5, (b) castor oil-in-DM5 (red) and (c) TOFA 26% oil-in-DM5 Pickering emulsions prepared using 2.0% w/w PSiMA$_{19}$-PBzMA$_{200}$ spheres in DM5 using a DM5 volume fraction of 0.50.

For Pickering emulsions, the total interfacial area that can be stabilized is directly proportional to the nanoparticle concentration.[5] Consequently, lowering the nanoparticle concentration at a fixed volume fraction of the droplet phase leads to the formation of fewer, larger droplets. This upturn in droplet diameter at lower nanoparticle concentrations is evident for the three oil-in-DM5 emulsions stabilised by PSiMA$_{19}$-PBzMA$_{200}$ shown in **Figure 5**. In contrast, if *in situ* nanoparticle dissociation had occurred, then a zero concentration dependence would be expected for the mean droplet diameter over this concentration range.[49] Thus, the data reported in **Figure 5** confirm that the PSiMA$_{19}$-PBzMA$_{200}$ nanoparticles do indeed survive high-shear homogenization and adsorb intact at the oil-oil interface. The corresponding optical micrographs obtained for these experiments are shown in **Figure S2**.

Pyrene-labeled nanoparticles were prepared to provide further evidence for their presence at the surface of the oil droplets. This was achieved by esterification of the carboxylic acid end-group on the PSiMA$_{19}$ stabilizer chains using 1-hydroxymethylpyrene according to **Scheme 2**.
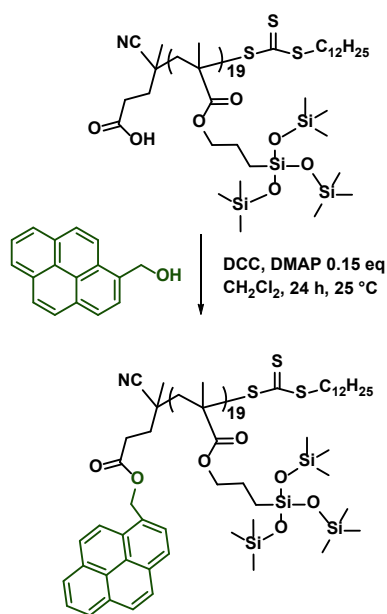
Scheme 2. Reaction scheme for the esterification of the carboxylic acid end-group on the PSiMA$_{19}$ precursor with 1-hydroxymethylpyrene using carbodiimide coupling chemistry.

After purification by precipitation into excess methanol, ^{1}H NMR analysis indicated that 30 mol% of the carboxylic acid end-groups had been converted into the corresponding ester (see **Figure S3**). This pyrene-functionalized PSiMA$_{19}$ precursor was then chain-extended via RAFT dispersion polymerization of BzMA in DM5 to produce fluorescent PSiMA$_{19}$-PBzMA$_{200}$ nanoparticles (see **Figure 6a**). **Figure 6b** shows a fluorescence micrograph recorded for a castor oil-in-DM5 Pickering emulsion prepared with such pyrene-labeled nanoparticles. This image confirms that these nanoparticles are indeed adsorbed at the castor oil/DM5 interface, as expected for a Pickering emulsion.
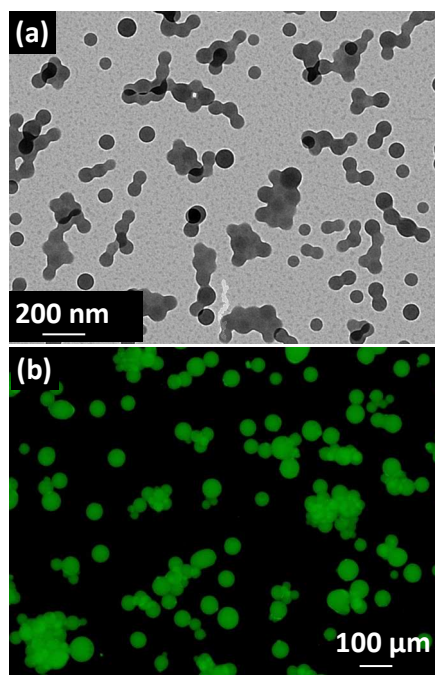
Figure 6. (a) TEM image recorded for pyrene-functionalized PSiMA$_{19}$-PBzMA$_{200}$ spheres prepared in DM5. (b) Fluorescence micrograph recorded for a castor oil-in-DM5 Pickering emulsion prepared using the nanoparticles shown in (a). Conditions: 0.75% w/w dispersion of PSiMA$_{19}$-PBzMA$_{200}$ spheres in DM5 prior to emulsification; high-shear homogenization was conducted at 7 500 rpm for 2 min at 20 °C; DM5 volume fraction = 0.50.

One of the primary mechanisms of emulsion instability is Ostwald ripening.[71] This is a spontaneous process whereby larger droplets grow at the expense of smaller ones because the former droplets are more thermodynamically stable. In emulsions, this occurs by diffusion of molecules from smaller droplets through the continuous phase into larger droplets. To investigate whether the oil-in-oil Pickering emulsions described herein suffered from Ostwald ripening, the mean droplet diameter was monitored over time for the castor oil-in-DM5, TOFA (26%) oil-in-DM5 and sunflower oil-in-DM5 emulsions, with each emulsion being prepared using 2.0% w/w PSiMA$_{19}$-PBzMA$_{200}$ spheres. According to **Figure 7**, both castor oil-in-DM5 and TOFA (26%) oil-in-DM5 emulsions remain stable for at least four weeks during storage at 20 °C, because there is no discernible increase in mean droplet diameter over this time period. On the other hand, the mean droplet diameter of the sunflower oil-in-DM5 emulsion increased from 32 ± 12 μm to 50 ± 13 μm over the same four-week time scale. Moreover, the cube of the droplet radius increased approximately linearly over time (see

Figure S4). This suggests that the background solubility of sunflower oil in DM5 is appreciably higher

than that of either castor oil or TOFA 26% oil, which leads to Ostwald ripening.[25] Given that TOFA

26% oil contains a significant proportion of rosin acid[72] and castor oil contains some hydroxyl

functionality,[73] the observed differences in long-term emulsion stability seem to be physically
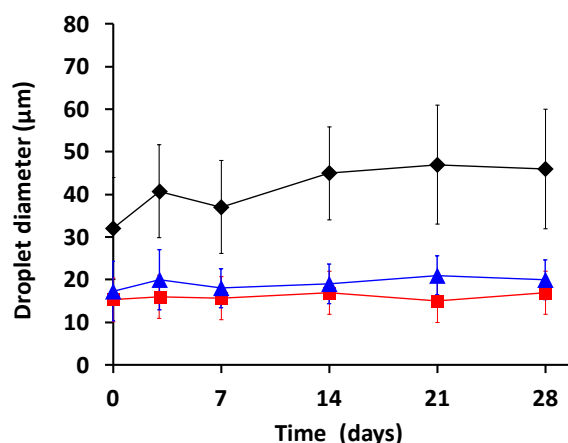
reasonable.

Figure 7. Number-average droplet diameter (as determined by digital image analysis of optical micrographs) observed over time for the sunflower oil-in-DM5 (black diamonds) castor oil-in-DM5 (red squares) and TOFA 26% oil-in-DM5 (blue triangles) Pickering emulsions. Each emulsion was prepared using 2.0% w/w $PSiMA_{19}$-$PBzMA_{200}$ spheres at a fixed DM5 volume fraction of 0.50. [N.B. Error bars correspond to one standard deviation of the droplet diameter, rather than indicating the experimental error].

Thus far, the $PSiMA_{19}$-$PBzMA_{200}$ spheres have been shown to be effective Pickering emulsifiers for

bio-sourced oil-in-DM5 emulsions prepared using either castor, sunflower or TOFA 26% oil.

However, seven out of the ten oils did not produce stable emulsions. To improve the Pickering

emulsifier performance of PSiMA-stabilized nanoparticles, LMA was statistically copolymerized with

BzMA when preparing the core-forming block. Given that PLMA is soluble in most of these bio-

sourced oils, this structural modification was anticipated to increase the nanoparticle wettability

with respect to the droplet phase. In principle, an alternative approach would be to statistically

copolymerize LMA with SiMA to modify the steric stabilizer block. However, this would most likely

have an adverse effect on the colloidal stability of the resulting nanoparticles because DM5 is only a

marginal solvent for PLMA. Moreover, when attemping to prepare PLMA-PBzMA nanoparticles

directly in DM5, complete loss of colloidal stability was always observed (data not shown). Hence

three new examples of PSiMA$_{19}$-stabilized diblock copolymer nanoparticles were synthesized with

P(BzMA-*stat*-LMA) core-forming blocks comprising 5.0, 12.5 or 18 mol% LMA, see **Table 2**. TEM

analysis confirmed that well-defined spheres were obtained in each case (see **Figure S5**).

Table 2. Summary of target diblock copolymer compositions, comonomer conversions, DLS and GPC data obtained for three examples of PSiMA-P(BzMA-*stat*-LMA) (denoted as S$_{19}$-(B$_x$-*stat*-L$_y$) for brevity) diblock copolymer nanoparticles prepared with varying proportions of LMA within the core-forming block.

Target diblock copolymer composition	Comonomer conversion / %[a]	LMA content within core-forming block (mol %)	DLS		GPC[b]	
			Z-average diameter / nm	PDI	M$_n$ / g mol^{-1}	M$_w$/M$_n$
S$_{19}$-(B$_{190}$-*stat*-L$_{10}$)	99	5.0	130	0.07	44,600	2.06
S$_{19}$-(B$_{175}$-*stat*-L$_{25}$)	99	12.5	147	0.07	55,200	1.60
S$_{19}$-(B$_{164}$-*stat*-L$_{36}$)	99	18.0	210	0.10	76,100	2.10

A series of oil-in-DM5 Pickering emulsions were prepared employing the ten oils shown in **Figure 2**

using each of the three types of LMA-modified nanoparticles summarized in **Table 2**. For each

emulsion, the nanoparticle concentration was 2.0% w/w and the DM5 volume fraction was 0.50. For

the PSiMA$_{19}$-P(BzMA$_{190}$-*stat*-LMA$_{10}$) nanoparticles, five of the ten oil-in-oil emulsions remained stable

after standing for two months at 20 °C (**Figure 8**) compared with just three emulsions when using

PSiMA$_{19}$-PBzMA$_{200}$ nanoparticles. In each case, optical microscopy studies confirmed the presence of

well-defined spherical droplets, and each emulsion was readily dispersible in excess DM5, indicating

that DM5 was the continuous phase. Close inspection of **Figure 8c** confirms that some of the

sunflower oil-in-DM5 droplets appear to be wrinkled. This suggests emulsion instability owing to

droplet shrinkage, as reported by Datta et al.[74] This is consistent with our observation that

sunflower oil appears to have a higher background solubility in DM5. If partial dissolution of the

sunflower oil in the DM5 continuous phase occurs, this would reduce the overall droplet volume and

give rise to buckling of the particle-laden interface. Furthermore, inspecting **Figure 8e**, some of the

linseed oil droplets appear to be elongated and non-spherical. Such behavior has been well-

documented in the literature and suggests some degree of arrested droplet coalescence.[75] Finally, inspecting Figure 8f, there is evidence of the formation of multiple emulsions, or droplets within droplets. This observation seems reasonable given the relatively high nanoparticle concentration (2% w/w) and is consistent with previous reports.[76] Overall, this set of experiments suggests that incorporation of even relatively small amounts of LMA comonomer into the nanoparticle cores can significantly influence their Pickering emulsifier performance.
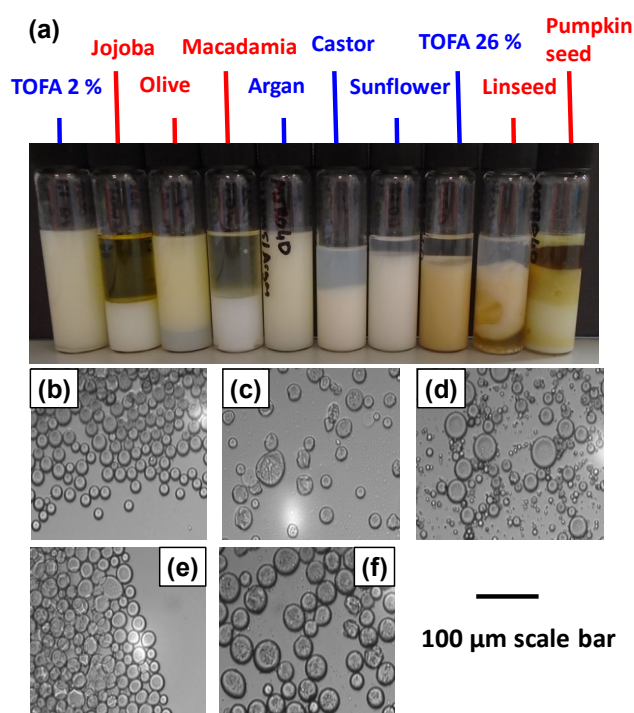

Figure 8. (a) Digital photograph of various oil-in-DM5 Pickering emulsions prepared using a 2.0% w/w dispersion of PSiMA$_{19}$-P(BzMA$_{190}$-*stat*-LMA$_{10}$) spheres in DM5 recorded after storage for two months at 20 °C. In each case, the DM5 volume fraction was 0.50 and the PSiMA$_{19}$-P(BzMA$_{190}$-*stat*-LMA$_{10}$) concentration was 2.0% w/w. The five emulsions that remained stable after two months are indicated in blue, whereas those that exhibited (partial) phase separation are shown in red. Representative optical micrographs for the five stable emulsions are also shown: (b) TOFA 26% oil-in-DM5, (c) sunflower oil-in-DM5, (d) castor oil-in-DM5, (e) argan oil-in-DM5 and (f) TOFA 2% oil-in-DM5 emulsions.

Next, the PSiMA$_{19}$-P(BzMA$_{174}$-*stat*-LMA$_{25}$) spheres were evaluated using the same conditions employed for **Figure 8** (see **Figure 9**). Clearly, these LMA-modified nanoparticles can stabilize a much wider range of oil-in-oil emulsions than the PSiMA$_{19}$-PBzMA$_{200}$ spheres. More specifically, only the jojoba oil-in-DM5 emulsion was judged to be unstable after two months. It is not immediately

obvious why this particular emulsion is unstable, because each of the oils used in this study are composed of similar compounds, i.e. medium and long-chain triglycerides.
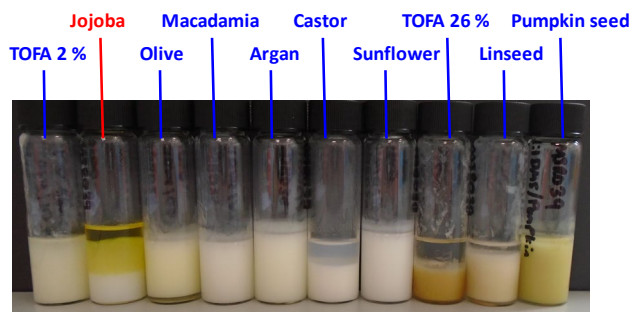

Figure 9. Digital photograph of various oil-in-DM5 Pickering emulsions prepared using a 2.0% w/w dispersion of PSiMA$_{19}$-P(BzMA$_{174}$-*stat*-LMA$_{25}$) spheres in DM5 recorded after storage for two months at 20 °C. In each case, the DM5 volume fraction was 0.50 and the PSiMA$_{19}$-P(BzMA$_{175}$-*stat*-LMA$_{25}$) concentration was 2.0% w/w. Emulsions that remained stable after two months are indicated in blue, whereas the single jojoba oil-based emulsion that underwent phase separation over this time period is shown in red.

One possible explanation for these observations is that Ostwald ripening is more significant for jojoba oil-in-DM5 emulsions than it is for the other nine oils. This is a plausible hypothesis because jojoba oil is primarily composed of triglycerides of 11-eicosenoic acid, which is an unsaturated C$_{20}$ chain. In contrast, the other bio-sourced oils are composed of triglycerides with unsaturated C$_{16-18}$ chains. Thus jojoba oil is somewhat less polar and therefore may have a higher background solubility in DM5. For the nine emulsions that remained stable after two months, optical microscopy studies confirmed the presence of well-defined droplets in each case (**Figure 10**). In addition, these emulsions proved to be readily dispersible in excess DM5, confirming that DM5 was the continuous phase in each case. Some of the linseed oil droplets shown in **Figure 10** appear to be non-spherical and somewhat elongated, which suggests arrested droplet coalescence.[75] Moreover, multiple emulsions appear to be formed in the case of the TOFA 2% oil and TOFA 26% oil formulations.
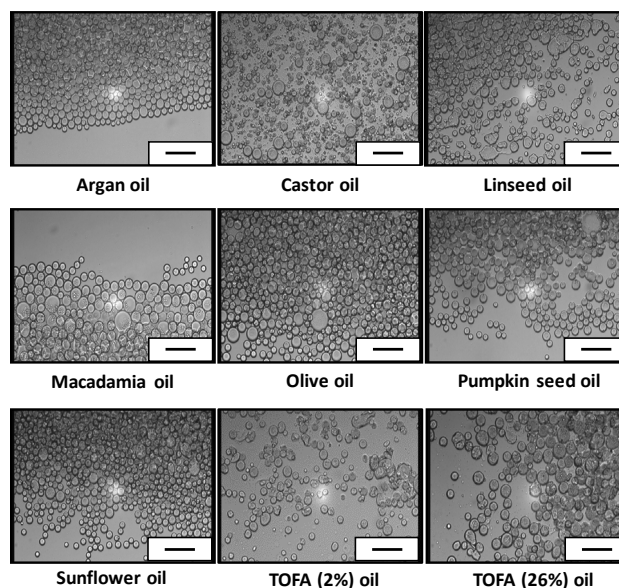
Figure 10. Optical micrographs recorded for the nine stable Pickering emulsions shown in **Figure 9.** In each case the scale bar corresponds to 100 μm.

Perhaps surprisingly, increasing the LMA content of the nanoparticle cores up to 18 mol% resulted in a significant *reduction* in emulsion stability (data not shown). Thus phase separation was observed for the TOFA 2%, TOFA 26% and jojoba oils, while using the remaining seven oils merely led to the formation of viscous pastes. These observations suggest that an *optimum* LMA content is required to achieve maximum Pickering emulsifier performance for such nanoparticles.

Conclusions

PSiMA$_{19}$-PBzMA$_{200}$ spherical nanoparticles can be prepared directly within a low-viscosity silicone oil (DM5). Such nanoparticles act as efficient Pickering stabilizers for oil-in-oil emulsions, where the droplet phase comprises either castor oil, sunflower oil, or TOFA 26% oil and the DM5 forms the continuous phase. When used at a copolymer concentration of 2.0% w/w, such nanoparticles can stabilize Pickering emulsions for at least two months, as confirmed by visual inspection and optical microscopy. Furthermore, the carboxylic acid end-groups located on the PSiMA stabilizer block enable convenient fluorescent labeling of the nanoparticles using pyrene, facilitating fluorescence microscopy studies of the resulting nanoparticle-stabilized castor oil-in-DM5 emulsions. Such

experiments confirm the presence of the PSiMA$_{19}$-PBzMA$_{200}$ nanoparticles adsorbed at the castor oil/DM5 interface.

A series of TOFA 26% oil-in-DM5, castor oil-in-DM5 or sunflower oil-in-DM5 emulsions were prepared by systematically varying the PSiMA$_{19}$-PBzMA$_{200}$ concentration. These sterically-stabilized nanoparticles remain intact at the interface during homogenization, rather than undergoing dissociation to form individual diblock copolymer chains, which is consistent with similar block copolymer nanoparticles[77]. The mean droplet diameter was monitored over time for these three emulsions in order to investigate whether these emulsions suffered from Ostwald ripening on ageing[71,78]. Initially, Ostwald ripening was indeed observed for the sunflower-in-DM5 emulsions when aged at 20 °C, but no further increase in droplet diameter occurred after approximately three weeks. In contrast, the castor oil-in-DM5 and TOFA 26%-in-DM5 emulsions exhibited no detectable Ostwald ripening when aged for one month at 20 °C.

Finally, PSiMA$_{19}$-based nanoparticles comprising a P(BzMA-*stat*-LMA) copolymer core-forming block can also act as a Pickering emulsifier. For an LMA content of 12.5 mol %, such nanoparticles can stabilize a significantly broader range of bio-sourced oils as the internal (droplet) phase. However, when the core comprises 18 mol % LMA, the corresponding Pickering emulsions become highly aggregated and unstable. This suggests that an optimum LMA content is required to achieve optimal Pickering emulsifier performance. This finding is in good agreement with previous literature on copolymer surfactant-stabilized emulsions[79] whereby the copolymer architecture and composition were found to be critical parameters in determining emulsion stability.

Supporting Information

UV spectra for the CDCP RAFT agent, density measurements for the various bio-sourced oils,

^{1}H NMR spectra for the pyrene-functionalized $PSiMA_{19}$ precursor, additional optical

micrographs and TEM images.

Author ORCID IDs

M. J. Rymaruk: 0000-0002-6622-6251

S. P. Armes: 0000-0002-8289-6351

References

[1]   J. Israelachvili, Intermolecular & Surface Forces, 2nd ed., Academic Press, London, 1991.

[2]   P.J. Wilde, Interfaces: their role in foam and emulsion behaviour, Curr. Opin. Colloid Interface Sci. 5 (2000) 176–181. https://doi.org/10.1016/S1359-0294(00)00056-X.

[3]   A. Kabalnov, Thermodynamic and theoretical aspects of emulsions and their stability, Curr. Opin. Colloid Interface Sci. 3 (1998) 270–275. https://doi.org/10.1016/S1359-0294(98)80071-X.

[4]   P. Finkle, H.D. Draper, J.H. Hildebrand, The Theory of Elmusification, J. Am. Chem. Soc. 45 (1923) 2780–2788. https://doi.org/10.1021/ja01665a002.

[5]   B.P. Binks, Particles as surfactants—similarities and differences, Curr. Opin. Colloid Interface Sci. 7 (2002) 21–41. https://doi.org/10.1016/S1359-0294(02)00008-0.

[6]   W.D. Bancroft, The Theory of Emulsification, V, J. Phys. Chem. 17 (1913) 501–519. https://doi.org/10.1021/j150141a002.

[7]   W.D. Bancroft, The Theory of Emulsification, VI, J. Phys. Chem. 19 (1914) 275–309.

https://doi.org/10.1021/j150157a002.

[8]   A. Pouchelon, D. Chatenay, J. Meunier, D. Langevin, Origin of low interfacial tensions in systems involving microemulsion phases, J. Colloid Interface Sci. 82 (1981) 418–422. https://doi.org/10.1016/0021-9797(81)90383-0.

[9]   R. Aveyard, B.P. Binks, S. Clark, J. Mead, Interfacial tension minima in oil–water–surfactant systems. Behaviour of alkane–aqueous NaCl systems containing aerosol OT, J. Chem. Soc. Faraday Trans. 1 Phys. Chem. Condens. Phases. 82 (1986) 125–142. https://doi.org/10.1039/f19868200125.

[10]   E.J. Burcik, The rate of surface tension lowering and its role in foaming, J. Colloid Sci. 5 (1950) 421–436. https://doi.org/10.1016/0095-8522(50)90034-1.

[11]   J.P. Hsu, A. Nacu, Behavior of soybean oil-in-water emulsion stabilized by nonionic surfactant, J. Colloid Interface Sci. 259 (2003) 374–381. https://doi.org/10.1016/S0021-9797(02)00207-2.

[12]   F. Opawale, D. Burgess, Influence of Interfacial Properties of Lipophilic Surfactants on Water-in-Oil Emulsion Stability, J. Colloid Interface Sci. 197 (1998) 142–50. https://doi.org/10.1006/jcis.1997.5222.

[13]   L.-I. Atanase, G. Riess, Block copolymers as polymeric stabilizers in non-aqueous emulsion polymerization, Polym. Int. 60 (2011) 1563–1573. https://doi.org/10.1002/pi.3137.

[14]   T. Tamura, Y. Kaneko, M. Ohyama, Dynamic Surface Tension and Foaming Properties of Aqueous Polyoxyethylene n-Dodecyl Ether Solutions, J. Colloid Interface Sci. 173 (1995) 493–499. https://doi.org/10.1006/jcis.1995.1351.

[15]   C. Hill, J. Eastoe, Foams: From nature to industry, Adv. Colloid Interface Sci. 247 (2017) 496–513. https://doi.org/10.1016/j.cis.2017.05.013.

[16]   W. Ramsden, Separation of Solids in the Surface-Layers of Solutions and "Suspensions" (Observations on Surface-Membranes, Bubbles, Emulsions, and Mechanical Coagulation). --Preliminary Account, Proc. R. Soc. London. 72 (1903) 156–164. https://doi.org/10.1098/rspl.1903.0034.

[17]   S.U. Pickering, CXCVI.—Emulsions, J. Chem. Soc., Trans. 91 (1907) 2001–2021. https://doi.org/10.1039/CT9079102001.

[18]   R. Aveyard, B.P. Binks, J.H. Clint, Emulsions stabilised solely by colloidal particles, Adv. Colloid Interface Sci. 100–102 (2003) 503–546. https://doi.org/10.1016/S0001-8686(02)00069-6.

[19]   B.P. Binks, Colloidal Particles at a Range of Fluid–Fluid Interfaces, Langmuir. 33 (2017) 6947–6963. https://doi.org/10.1021/acs.langmuir.7b00860.

[20]   B.P. Binks, C.P. Whitby, Silica Particle-Stabilized Emulsions of Silicone Oil and Water: Aspects of Emulsification, Langmuir. 20 (2004) 1130–1137. https://doi.org/10.1021/la0303557.

[21]   E.M. Herzig, K.A. White, A.B. Schofield, W.C.K. Poon, P.S. Clegg, Bicontinuous emulsions stabilized solely by colloidal particles, Nat. Mater. 6 (2007) 966–971. https://doi.org/10.1038/nmat2055.

[22]   D.J. French, P. Taylor, J. Fowler, P.S. Clegg, Making and breaking bridges in a Pickering emulsion, J. Colloid Interface Sci. 441 (2015) 30–38. https://doi.org/10.1016/j.jcis.2014.11.032.

[23]   Y. Liu, X. Chen, R. Wang, J.H. Xin, Polymer microspheres stabilized by titania nanoparticles, Mater. Lett. 60 (2006) 3731–3734. https://doi.org/10.1016/j.matlet.2006.03.098.

[24] R. Aveyard, B.P. Binks, P.D.I. Fletcher, C.E. Rutherford, Measurement monodisperse of contact angles of spherical particles with surfactant solutions, Colloids Surfaces A Physicochem. Eng. Asp. 83 (1994) 89–98.

[25] N.P. Ashby, B.P. Binks, Pickering emulsions stabilised by Laponite clay particles, Phys. Chem. Chem. Phys. 2 (2000) 5640–5646. https://doi.org/10.1039/b007098j.

[26] S.A.F. Bon, P.J. Colver, Pickering Miniemulsion Polymerization Using Laponite Clay as a Stabilizer, Langmuir. 23 (2007) 8316–8322. https://doi.org/10.1021/la701150q.

[27] J.H. Schulman, J. Leja, Control of contact angles at the oil-water-solid interfaces. Emulsions stabilized by solid particles (BaSO4), Trans. Faraday Soc. 50 (1954) 598–605. https://doi.org/10.1039/tf9545000598.

[28] B. Madivala, S. Vandebril, J. Fransaer, J. Vermant, Exploiting particle shape in solid stabilized emulsions, Soft Matter. 5 (2009) 1717–1727. https://doi.org/10.1039/b816680c.

[29] Q. Luo, Y. Wang, E. Yoo, P. Wei, E. Pentzer, Ionic Liquid-Containing Pickering Emulsions Stabilized by Graphene Oxide-Based Surfactants, Langmuir. 34 (2018) 10114–10122. https://doi.org/10.1021/acs.langmuir.8b02011.

[30] R. Van Hooghten, L. Imperiali, V. Boeckx, R. Sharma, J. Vermant, Rough nanoparticles at the oil–water interfaces: their structure, rheology and applications, Soft Matter. 9 (2013) 10791–10798. https://doi.org/10.1039/c3sm52089g.

[31] I. Kalashnikova, H. Bizot, P. Bertoncini, B. Cathala, I. Capron, Cellulosic nanorods of various aspect ratios for oil in water Pickering emulsions, Soft Matter. 9 (2013) 952–959. https://doi.org/10.1039/C2SM26472B.

[32] M. Andresen, P. Stenius, Water-in-oil Emulsions Stabilized by Hydrophobized Microfibrillated Cellulose, J. Dispers. Sci. Technol. 28 (2007) 837–844. https://doi.org/10.1080/01932690701341827.

[33] I. Kalashnikova, H. Bizot, B. Cathala, I. Capron, New pickering emulsions stabilized by bacterial cellulose nanocrystals, Langmuir. 27 (2011) 7471–7479. https://doi.org/10.1021/la200971f.

[34] B.P. Binks, S.O. Lumsdon, Pickering emulsions stabilized by monodisperse latex particles: Effects of particle size, Langmuir. 17 (2001) 4540–4547. https://doi.org/10.1021/la0103822.

[35] R. Aveyard, J.H. Clint, D. Nees, V.N. Paunov, Compression and structure of monolayers of charged latex particles at air/water and octane/water interfaces, Langmuir. 16 (2000) 1969–1979. https://doi.org/10.1021/la990887g.

[36] S. Fujii, E.S. Read, B.P. Binks, S.P. Armes, Stimulus-responsive emulsifiers based on nanocomposite microgel particles, Adv. Mater. 17 (2005) 1014–1018. https://doi.org/10.1002/adma.200401641.

[37] M. Destribats, M. Rouvet, C. Gehin-Delval, C. Schmitt, B.P. Binks, Emulsions stabilised by whey protein microgel particles: towards food-grade Pickering emulsions, Soft Matter. 10 (2014) 6941–6954. https://doi.org/10.1039/C4SM00179F.

[38] M.S. Manga, O.J. Cayre, R.A. Williams, S. Biggs, D.W. York, Production of solid-stabilised emulsions through rotational membrane emulsification: influence of particle adsorption kinetics, Soft Matter. 8 (2012) 1532–1538. https://doi.org/10.1039/C1SM06547E.

[39] T. Chen, P.J. Colver, S.A.F. Bon, Organic–Inorganic Hybrid Hollow Spheres Prepared from TiO2-Stabilized Pickering Emulsion Polymerization, Adv. Mater. 19 (2007) 2286–2289. https://doi.org/10.1002/adma.200602447.

[40] M. Williams, S.P. Armes, D.W. York, Clay-Based Colloidosomes, Langmuir. 28 (2012) 1142–1148. https://doi.org/10.1021/la2046405.

[41] S. Cauvin, P.J. Colver, S.A.F. Bon, Pickering Stabilized Miniemulsion Polymerization: Preparation of Clay Armored Latexes, Macromolecules. 38 (2005) 7887–7889. https://doi.org/10.1021/ma051070z.

[42] A.G. Cunha, J.B. Mougel, B. Cathala, L. a. Berglund, I. Capron, Preparation of double pickering emulsions stabilized by chemically tailored nanocelluloses, Langmuir. 30 (2014) 9327–9335. https://doi.org/10.1021/la5017577.

[43] O.D. Velev, K. Furusawa, K. Nagayama, Assembly of latex particles by using emulsion droplets as templates .1. Microstructured hollow spheres, Langmuir. 12 (1996) 2374–2384. https://doi.org/10.1021/la9506786.

[44] O.D. Velev, K. Furusawa, K. Nagayama, Assembly of latex particles by using emulsion droplets as templates .2. Ball-like and composite aggregates, Langmuir. 12 (1996) 2385–2391. https://doi.org/10.1021/la950679y.

[45] O.J. Cayre, S. Biggs, Hollow microspheres with binary porous membranes from solid-stabilised emulsion templates, J. Mater. Chem. 19 (2009) 2724–2728. https://doi.org/10.1039/b820842e.

[46] L.N. Arnaudov, O.J. Cayre, M. a C. Stuart, S.D. Stoyanov, V.N. Paunov, Measuring the three-phase contact angle of nanoparticles at fluid interfaces, Phys. Chem. Chem. Phys. 12 (2010) 328–331. https://doi.org/10.1039/b917353f.

[47] H. Maeda, M. Okada, S. Fujii, Y. Nakamura, T. Furuzono, Pickering-type water-in-oil-in-water multiple emulsions toward multihollow nanocomposite microspheres., Langmuir. 26 (2010) 13727–31. https://doi.org/10.1021/la102529d.

[48] V.J. Cunningham, A.M. Alswieleh, K.L. Thompson, M. Williams, G.J. Leggett, S.P. Armes, O.M. Musa, Poly(glycerol monomethacrylate)–Poly(benzyl methacrylate) Diblock Copolymer Nanoparticles via RAFT Emulsion Polymerization: Synthesis, Characterization, and Interfacial Activity, Macromolecules. 47 (2014) 5613–5623. https://doi.org/10.1021/ma501140h.

[49] K.L. Thompson, C.J. Mable, A. Cockram, N.J. Warren, V.J. Cunningham, E.R. Jones, R. Verber, S.P. Armes, Are block copolymer worms more effective Pickering emulsifiers than block copolymer spheres?, Soft Matter. 10 (2014) 8615–8626. https://doi.org/10.1039/C4SM01724B.

[50] P.F. Noble, O.J. Cayre, R.G. Alargova, O.D. Velev, V.N. Paunov, Fabrication of "hairy" colloidosomes with shells of polymeric microrods, J. Am. Chem. Soc. 126 (2004) 8092–8093. https://doi.org/10.1021/ja047808u.

[51] K.L. Thompson, L.A. Fielding, O.O. Mykhaylyk, J.A. Lane, M.J. Derry, S.P. Armes, Vermicious thermo-responsive Pickering emulsifiers, Chem. Sci. 6 (2015) 4207–4214. https://doi.org/10.1039/C5SC00598A.

[52] P.N. Sturzenegger, U.T. Gonzenbach, S. Koltzenburg, L.J. Gauckler, Controlling the formation of particle-stabilized water-in-oil emulsions, Soft Matter. 8 (2012) 7471–7479. https://doi.org/10.1039/c2sm25176k.

[53] S. Levine, B.D. Bowen, S.J. Partridge, Stabilization of emulsions by fine particles I. Partitioning of particles between continuous phase and oil/water interface, Colloids and Surfaces. 38 (1989) 325–343. https://doi.org/10.1016/0166-6622(89)80271-9.

[54]   B.P. Binks, S.O. Lumsdon, Catastrophic Phase Inversion of Water-in-Oil Emulsions Stabilized by Hydrophobic Silica, Langmuir. 16 (2000) 2539–2547. https://doi.org/10.1021/la991081j.

[55]   B.P. Binks, A.T. Tyowua, Oil-in-oil emulsions stabilised solely by solid particles, Soft Matter. 12 (2016) 876–887. https://doi.org/10.1039/C5SM02438B.

[56]   A.T. Tyowua, S.G. Yiase, B.P. Binks, Double oil-in-oil-in-oil emulsions stabilised solely by particles, J. Colloid Interface Sci. 488 (2017) 127–134. https://doi.org/10.1016/j.jcis.2016.10.089.

[57]   Z. Rozynek, R. Bielas, A. Józefczak, Efficient formation of oil-in-oil Pickering emulsions with narrow size distributions by using electric fields, Soft Matter. 14 (2018) 5140–5149. https://doi.org/10.1039/C8SM00671G.

[58]   B.J. Rodier, A. de Leon, C. Hemmingsen, E. Pentzer, Polymerizations in oil-in-oil emulsions using 2D nanoparticle surfactants, Polym. Chem. 9 (2018) 1547–1550. https://doi.org/10.1039/C7PY01819C.

[59]   X. Lu, J.S. Katz, A.K. Schmitt, J.S. Moore, A Robust Oil-in-Oil Emulsion for the Nonaqueous Encapsulation of Hydrophilic Payloads, J. Am. Chem. Soc. 140 (2018) 3619–3625. https://doi.org/10.1021/jacs.7b11847.

[60]   S.L. Rizzelli, E.R. Jones, K.L. Thompson, S.P. Armes, Preparation of non-aqueous Pickering emulsions using anisotropic block copolymer nanoparticles, Colloid Polym. Sci. 294 (2016) 1–12. https://doi.org/10.1007/s00396-015-3785-3.

[61]   P.S. Clegg, E.M. Herzig, A.B. Schofield, S.U. Egelhaaf, T.S. Horozov, B.P. Binks, M.E. Cates, W.C.K. Poon, Emulsification of partially miscible liquids using colloidal particles: Nonspherical and extended domain structures, Langmuir. 23 (2007) 5984–5994. https://doi.org/10.1021/la063707t.

[62]   A.K.F. Dyab, L.A. Mohamed, F. Taha, Non-aqueous olive oil-in-glycerin (o/o) Pickering emulsions: Preparation, characterization and in vitro aspirin release, J. Dispers. Sci. Technol. 39 (2018) 890–900. https://doi.org/10.1080/01932691.2017.1406368.

[63]   A.M. Tawfeek, A.K.F. Dyab, H.A. Al-Lohedan, Synergetic Effect of Reactive Surfactants and Clay Particles on Stabilization of Nonaqueous Oil-in-Oil (o/o) Emulsions, J. Dispers. Sci. Technol. 35 (2014) 265–272. https://doi.org/10.1080/01932691.2013.769110.

[64]   A. Mikkelsen, K. Khobaib, F.K. Eriksen, K.J. Måløy, Z. Rozynek, Particle-covered drops in electric fields: drop deformation and surface particle organization, Soft Matter. 14 (2018) 5442–5451. https://doi.org/10.1039/C8SM00915E.

[65]   A. Mikkelsen, Z. Rozynek, Mechanical Properties of Particle Films on Curved Interfaces Probed through Electric Field-Induced Wrinkling of Particle Shells, ACS Appl. Mater. Interfaces. 11 (2019) 29396–29407. https://doi.org/10.1021/acsami.9b08045.

[66]   T. Kubiak, J. Banaszak, A. Józefczak, Z. Rozynek, Direction-Specific Release from Capsules with Homogeneous or Janus Shells Using an Ultrasound Approach, ACS Appl. Mater. Interfaces. 12 (2020) 15810–15822. https://doi.org/10.1021/acsami.9b21484.

[67]   A. Mikkelsen, Z. Rozynek, K. Khobaib, P. Dommersnes, J.O. Fossum, Transient deformation dynamics of particle laden droplets in electric field, Colloids Surfaces A Physicochem. Eng. Asp. 532 (2017) 252–256. https://doi.org/10.1016/j.colsurfa.2017.05.010.

[68]   R. Bielas, Z. Rozynek, T. Hornowski, A. Józefczak, Ultrasound control of oil-in-oil Pickering emulsions preparation, J. Phys. D. Appl. Phys. 53 (2020) 085301.

https://doi.org/10.1088/1361-6463/ab58a7.

[69] M.J. Rymaruk, C.T. O'Brien, S.L. Brown, C.N. Williams, S.P. Armes, RAFT Dispersion Polymerization of Benzyl Methacrylate in Silicone Oil Using a Silicone-Based Methacrylic Stabilizer Provides Convenient Access to Spheres, Worms, and Vesicles, Macromolecules. 53 (2020) 1785–1794. https://doi.org/10.1021/acs.macromol.9b02697.

[70] J.S. Trent, J.I. Scheinbeim, P.R. Couchman, Ruthenium tetraoxide staining of polymers for electron microscopy, Macromolecules. 16 (1983) 589–598. https://doi.org/10.1021/ma00238a021.

[71] P. Taylor, Ostwald ripening in emulsions, Colloids Surfaces A Physicochem. Eng. Asp. 99 (1995) 175–185. https://doi.org/10.1016/0927-7757(95)03161-6.

[72] A.L. Jones, R.W. Foreman, Liquid Thermal Diffusion of Tall Oil, Ind. Eng. Chem. 44 (1952) 2249–2253. https://doi.org/10.1021/ie50513a071.

[73] G.W. Priest, J.D. Von Mikusch, Composition and Analysis of Dehydrated Castor Oil, Ind. Eng. Chem. 32 (1940) 1314–1319. https://doi.org/10.1021/ie50370a010.

[74] S.S. Datta, H.C. Shum, D.A. Weitz, Controlled Buckling and Crumpling of Nanoparticle-Coated Droplets, Langmuir. 26 (2010) 18612–18616. https://doi.org/10.1021/la103874z.

[75] A.B. Pawar, M. Caggioni, R. Ergun, R.W. Hartel, P.T. Spicer, Arrested coalescence in Pickering emulsions, Soft Matter. 7 (2011) 7710. https://doi.org/10.1039/c1sm05457k.

[76] C.P. Whitby, R. Parthipan, Influence of particle concentration on multiple droplet formation in Pickering emulsions, J. Colloid Interface Sci. 554 (2019) 315–323. https://doi.org/10.1016/j.jcis.2019.07.017.

[77] K.L. Thompson, J.A. Lane, M.J. Derry, S.P. Armes, Non-aqueous Isorefractive Pickering Emulsions., Langmuir. 31 (2015) 4373–6. https://doi.org/10.1021/acs.langmuir.5b00630.

[78] P. Taylor, Ostwald ripening in emulsions, Adv. Colloid Interface Sci. 75 (1998) 107–163. https://doi.org/10.1016/S0001-8686(98)00035-9.

[79] N. Ezaki, Y. Watanabe, H. Mori, Nonaqueous Dispersion Formed by an Emulsion Solvent Evaporation Method Using Block–Random Copolymer Surfactant Synthesized by RAFT Polymerization, Langmuir. 31 (2015) 11399–11408. https://doi.org/10.1021/acs.langmuir.5b02358.